Published in final edited form as:
*Clin Neurophysiol*. 2001 October ; 112(10): 1781–1792.

# Transcranial magnetic stimulation coregistered with MRI: a comparison of a guided versus blind stimulation technique and its effect on evoked compound muscle action potentials

**Laverne D. Gugino**[a,*], **J. Rafael Romero**[a], **Linda Aglio**[a], **Debra Titone**[b], **Marcela Ramirez**[a], **Alvaro Pascual-Leone**[c], **Eric Grimson**[d], **Neil Weisenfeld**[d], **Ron Kikinis**[e], and **Martha-E. Shenton**[e,f]

[a]Department of Anesthesia, Brigham and Women's Hospital, Harvard Medical School, CWN-L1, 75 Francis Street, Boston, MA 02115, USA

[b]Psychology Research Laboratory, McLean Hospital, Harvard Medical School, 115 Mill Street, Belmont, MA 02174, USA

[c]Department of Neurology, Beth Israel Deaconess Medical Center, Harvard Medical School, 330 Brookline Avenue, Boston, MA 02215, USA

[d]MIT AI Laboratory, 545 Technology Square, Cambridge, MA 02139, USA

[e]Department of Radiology, Brigham and Women's Hospital, Harvard Medical School, 75 Francis Street, Boston, MA 02115, USA

[f]Clinical Neuroscience Division, Laboratory of Neuroscience, Boston VA Healthcare System, Brockton Division, Department of Psychiatry, Harvard Medical School, 940 Belmont Street, Brockton, MA 02301, USA

## Abstract

**Introduction and methods—**Compound muscle action potentials (CMAPs) elicited by transcranial magnetic stimulation (TMS) are characterized by enormous variability, even when attempts are made to stimulate the same scalp location. This report describes the results of a comparison of the spatial errors in coil placement and resulting CMAP characteristics using a guided and blind TMS stimulation technique. The former uses a coregistration system, which displays the intersection of the peak TMS induced electric field with the cortical surface. The latter consists of the conventional placement of the TMS coil on the optimal scalp position for activation of the first dorsal interossei (FDI) muscle.

**Results—**Guided stimulation resulted in significantly improved spatial precision for exciting the corticospinal projection to the FDI compared to blind stimulation. This improved precision of coil placement was associated with a significantly increased probability of eliciting FDI responses. Although these responses tended to have larger amplitudes and areas, the coefficient of variation between guided and blind stimulation induced CMAPs did not significantly differ.

**Conclusion—**The results of this study demonstrate that guided stimulation improves the ability to precisely revisit previously stimulated cortical loci as well as increasing the probability of eliciting TMS induced CMAPs. Response variability, however, is due to factors other than coil placement.

* Corresponding author. Tel.: +1-617-732-8222; fax: +1-617-277-2192. vern@zeus.bwh.harvard.edu (L.D. Gugino).

**Keywords**

Transcranial magnetic stimulation and coregistration system; Compound muscle action potentials; Variability

## 1. Introduction

Transcranial magnetic stimulation (TMS) was developed and introduced in 1985 by Barker and coworkers as a safe and painless means for stimulating the human cortex (Barker et al., 1985). When TMS is applied to restricted loci on the scalp it elicits compound muscle action potentials (CMAPs) from discrete skeletal muscles. Several investigators have produced maps of the location and extent of the motor cortical outputs. This has been done by plotting the TMS elicited CMAPs' amplitude or area as a function of stimulated scalp areas (Levy et al., 1991; Cohen et al., 1991a; Wassermann et al., 1992; Brasil-Neto et al., 1992a; Mortifee et al., 1994; Thickbroom et al., 1999). The studies of both normal and pathological motor control as well as brain plasticity have resulted from the utilization of TMS in medical research (Levy et al., 1990; Cohen et al., 1991a,b, Cohen et al., 1993; Traversa et al., 1997). However, knowledge of the specific cortical region stimulated by using focal TMS (as opposed to the scalp location of the coil) may in addition lead to the creation of functional cortical maps useful for preoperative evaluation for planning neurosurgical procedures near eloquent cortical areas (Krings et al., 1997a; Grimson et al., 1999).

One problem common to TMS studies is the enormous variability of the CMAPs. This variability has been attributed to numerous neurophysiological factors that have a potential impact on membrane excitability levels of cortical and/or spinal cord neurons (Brasil-Neto et al., 1992a; Mortifee et al., 1994; Fadiga et al., 1995; Izumi et al., 1995; Brouwer and Qiao 1995; Nielsen and Petersen, 1995; Ellaway et al., 1998). It is to be noted that most studies have not taken into account the degree of precision attainable in placing and repositioning the TMS stimulating coil on the scalp for exciting restricted cortical surface loci. Specifically, several studies have shown that at the microstimulation level, motor cortex organization consists of spatially discrete redundant clusters of neurons primarily responsible for the activation of specific lower motoneurons (Asanuma et al., 1976; Asanuma, 1981; Cheney and Fetz, 1984). Nevertheless, neurons on the fringe of these clusters show divergence with respect to lower motor neurons in the spinal cord. Therefore, as the focus of neurostimulation is remote from the coil, even small errors in its placement on the scalp might lead to a difference in the neurons excited in cortical neuronal clusters and thereby contribute to the variability of CMAPs.

In a previous report we introduced a coregistration system, which can be used to relate actual scalp locations to virtual cortical surface loci below (Ettinger et al., 1996). The virtual cortical surface is derived from a 3-dimensional brain reconstructed from magnetic resonance images (MRIs). We assume that the peak electric field induced by a figure of 8 coil is generated along an axis that goes through the center and is perpendicular to the plane defined by the figure of 8 coil (Cohen et al., 1990; Cohen and Cuffin 1991). Using this assumption, the coregistration system is capable of tracking the peak stimulating electric field as it intersects the underlying cortical surface (Gugino et al., 1999).

Our hypothesis was that precise tracking of the location and orientation of a TMS coil relative to the cortical area intersected by the assumed peak electric field would allow us to reproducibly perform stimulation of targeted neocortical areas. In addition, we wanted to compare the results of guided stimulation to conventional blind TMS where the experimenter relies on a marked grid drawn on a cap placed on a subject's head for determining placement of the coil. A

subsidiary goal of this study was to evaluate differences in the variability of TMS induced CMAPs using a guided versus blind stimulation technique of increasing stimulus intensities.

## 2. Methods and materials

### 2.1. Subjects

Informed written consent was obtained from 5 subjects for this prospective study approved by the Human Research Committee and covered by an Investigational Device Exemption (IDE) from the Food and Drug Administration (FDA). The 5 subjects (4 males and one female) were normal volunteers aged 22–46 years. All of them were familiar with TMS. All were right handed according to the Edinburg Handedness inventory (Oldfield, 1974).

### 2.2. MRI acquisition

MRIs were acquired using a 1.5 T General Electric Sigma System scanner (General Electric Medical Systems, Milwaukee, WI, USA). MRI scanning parameters included a repetition time of 35 ms, an echo time of 5 ms, slice thickness of 1.5 mm, a field of view of 24 cm and an acquisition matrix of 256 × 256 voxels (192 phase-encoding steps with zero filling). A conjugate synthesis in combination with an interleaved acquisition resulted in 124 contiguous double-echo slices whose voxel dimensions were $0.9375 \times 0.9375 \times 1.5\ mm^3$. The construction of 3-dimensional MRI representations of each volunteer's head was carried out using in-house developed multistep algorithms (Shenton et al., 1995; Kapur et al., 1995; Ettinger et al., 1996).

### 2.3. Experimental setup

After MR scanning, subjects were positioned on a cot under the boom-mounted cameras of our optical tracking system (Fig. 1). Five light emitting diodes (LEDs) were attached to the skin, using adhesive tape, allowing the system to track the subject's head. Another set of LEDs was attached to the TMS coil, allowing tracking of the coil position relative to the subject. This setup allowed ‘free-hand movement’ of the TMS coil and comfortable positioning of the subject, without need for head fixation. A laser scanner, mentioned below, was attached and calibrated to the camera system.

### 2.4. Coregistration procedure

A coregistration system that utilizes a 3-dimensional reconstruction of a person's MRI of the brain, overlying scalp and face was used (for specific details see Ettinger et al., 1996). Briefly, coregistration is accomplished by first measuring the exact location of several hundred points on the skin surface of the patient's head and face using either a laser scanner or an optical tracking system (Image Guided Technologies, Inc., Boulder, CO, USA). The points are then used to perform a registration procedure to the skin surface extracted from the MRI data. This registration finds the optimal transformation between the actual skin points and the skin surface of the MRI reconstructed subject model. The result of these procedures is a virtual head in which the cortical surface is used for mapping studies.

Moreover, a display shows a line representing the intersection of the peak TMS induced electric field and the virtual cortical surface beneath the scalp (Fig. 2). The coregistration system can, therefore, be used in real time for guiding the placement of the coil in order to stimulate desired areas of the cortex. After the initial co-registration, the image is available instantaneously and is updated at a rate of approximately 5 times per second. As the operator moves the coil on the surface of the head, the line on the computer display moves relative to the brain surface. This allows the operator to control the placement of the TMS coil in order to stimulate target areas of the cortex.

### 2.5. Localization of the first dorsal interossei (FDI) cortical surface optimum site

After completing the coregistration, a planar 1 × 1 $cm^2$ grid whose dimensions were 9 × 9 $cm^2$, was tangentially displayed on the virtual cortical surface and scalp using a high-resolution monitor. The grid was projected onto the virtual cortical surface with its medial edge parallel to the inter-hemispheric fissure and the anterior edge placed anterior to the tip of the temporal lobe.

A figure of 8 coil (Magstim Company, Wales, UK). of 7.5 cm outer diameter was used for stimulation. The coil was connected to a Magstim Rapid Rate Magnetic Stimulator (Magstim Company, Wales, UK). capable of delivering single triggered biphasic current pulses having the contour of a damped cosine, with the second phase smaller than the first. The duration of each pulse is approximately 350 μs, with a rise time of approximately 80–100 μs. At full stimulation strength output, a 2.0 T magnetic pulse is generated.

The center of the figure of 8 coil (i.e. tracking point) was systematically placed at each intersection point of the grid projected onto the virtual cortical surface. This was guided by the optical tracking system.

The TMS at 85% of full stimulation strength was used for mapping the scalp and underlying cortical surface locations of the motor cortex. This stimulation strength was chosen, as previous experience had shown that it was greater than the motor threshold intensity for reliably eliciting responses from distal upper limb muscles (i.e. between 1.1 and 1.3 times resting motor threshold (rMT) in our subjects) (see Table 1). On the other hand, by using TMS intensities lower than 100%, less intracortical current spread would yield motor cortex surface maps focused on the lower threshold upper motor neurons (Pascual-Leone et al., 1994). The coil was oriented for inducing cortical currents perpendicular to the central sulcus, a direction shown to be optimal for activation of hand muscles (Brasil-Neto et al., 1992b).

Motor cortex localization criteria was based on the acquisition of TMS induced CMAPs from the contralateral FDI muscle. All recordings were acquired using silver–silver chloride stick on electrodes (3M, Red Dots™, St. Paul, MN, USA). placed in a muscle belly-tendon fashion with a ground on the left shoulder. Electrode impedance was less than 5 kω with a 2 kω or less inter-electrode difference for the recording channel. The recording parameters included a bandwidth of 10–10 000 Hz (3 db down), and a recording time window of 80 ms. The volunteers were trained to relax all muscles prior to stimulation. Three TMS stimuli were applied at each intersection point of the superimposed grid with an inter-stimulus interval of 30 s, until no responses were obtained. This defined the limits of the motor map. The CMAPs were recorded along with the stimulated grid point locations on both the virtual scalp and cortical surface for off-line analysis.

The optimal location was defined as the cortical surface locus giving the largest averaged amplitude CMAPs for the contralateral FDI muscle. This phase of the experiment lasted approximately 1.5 h for each subject.

Topographical maps were then constructed using CMAP amplitude data. The maximum CMAP amplitude was used for normalizing each averaged response. A 4-point interpolated color two-dimensional cortical surface and scalp map was then constructed for FDI responses using the normalized CMAP amplitudes as a function of their cortical surface location. The virtual maps for FDI were then inspected for determining the optimal stimulating scalp position as defined above (Fig. 3).

### 2.6. Variability study protocol

This phase attempted to compare the variability of FDI CMAPs acquired during two types of stimulation: blind and guided. The blind stimulation involved placement of the TMS coil on the scalp without visual feedback information concerning the underlying cortical surface location intersected by the induced electrical field. A tight fitting swimming cap was placed on each volunteer's head and the coil position where TMS produced the largest averaged FDI CMAPs (i.e. optimal scalp location) was marked. The center of the anterior edge of the figure of 8 coil was also marked while the coil was held on the optimal position, assuring that the center of the coil remained over the optimal site marked on the cap.

The rMT was determined starting with a suprathreshold intensity and decreasing stimulator output in steps of 2%. The rMT was defined as the lowest TMS intensity producing CMAPs with peak-to-peak amplitude of at least 100 μV in 5 out of 10 stimuli (Kiers et al., 1993; Nielsen, 1996a; Krings et al., 1997a; Triggs et al., 1999). A comparison of the rMT and the intensity used during this phase of the study is shown in Table 1. Next, each of the 4 different experimenters placed the coil on a subject's head with attention to maintaining the same coil position and orientation relative to the mark representing the center of the anterior edge of the figure of 8 coil. Each of the subjects was stimulated 15 times at threshold, at a stimulation strength half way between threshold and 100% strength, and at full (100%) stimulator output. These stimulation intensities were employed in order to evaluate the influence of stimulation intensity on acquired response variability, and are referred to in this report as the first, second and third power levels, respectively.

Guided stimulation followed the blind stimulation protocol to avoid any influence of repetitive coil placement aided by the guided system on the blind placement of the coil. This was accomplished by allowing each experimenter to visualize where the presumed elicited peak electric field intersected the virtual scalp and cortical surface location stimulated during a second series of 15 stimuli at the first, second and third power levels. The display also showed the twist angle of the coil (Fig. 2). The inter-stimulus interval was 30 s. Each experimenter applied a total of 45 stimuli during both blind and guided stimulation. In both, blind and guided conditions, the coil was removed after stimulation and replaced in the optimal location before the next trial. This phase of the experiment lasted approximately 3 h, with a 5 min transition between blind and guided conditions.

### 2.7. Analysis

All CMAPs were analyzed for (1) take off latency, (2) peak-to-peak amplitude, (3) area under the CMAP response curve between take off and recovery latency. The average of these response parameters across each group of stimuli was calculated as a function of stimulation intensity and blinded condition.

In order to determine if visually guided stimulation conferred any advantage over blinded stimulation, the distribution of cortical surface locations actually stimulated when placing the stimulating coil at the scalp or cortical surface optimal location was compared between the two conditions. Each coil stimulating location on the scalp and cortical surface was calculated by a distance along each of 3 mutually orthogonal axes whose vertex was set at the center of the 3-dimensional reconstructed MRI volume of each volunteer's head and underlying brain. Differences in the numerical descriptors, which defined the location where the stimulating coil's peak electric field intersected the scalp and cortical surface, were also calculated. These descriptors included both the Pythagorean distances between stimulated locations and the TMS coil twist angle. The difference in twist angle of the TMS coil between the initial coil orientation used for locating the FDI optimal location, and each subsequent stimulation trial was determined using a numerical method described by Horn (1987). This method is based on the

geometric premise that a single coil orientation (i.e. a stimulation trial orientation) in 3 dimensions can be brought into alignment with a second orientation (i.e. the initial TMS coil orientation) by using a single rotation around a certain axis. A comparison of the two orientations is accomplished by solving for the single rotation that must be made in order to bring the two coil orientations into register. The numerical method used gives both the angle and axis of rotation. The angle reported by this method was used for describing how well aligned the coil placements were for each stimulation. The values of these location descriptors were compared across blinded conditions using a repeated measure analysis of variance (ANOVA).

A repeated measure ANOVA was also used for comparing the derived parameters of the FDI CMAPs acquired during blind and guided stimulation, across all volunteers. To specifically investigate the effectiveness of MRI coregistration and the interaction of stimulus intensity, we manipulated whether the experimenters attempted to revisit a cortical optimal location using guided versus blind stimulation and crossed these two conditions with the 3 stimulating intensity levels (i.e. first, second, and third power levels). Thus, blindness and intensity were both within subject variables.

## 3. Results

The first hypothesis, that the image guided system, compared to blind stimulation, would improve the accuracy revisiting a known optimum cortical location during TMS, was confirmed. The ANOVAs revealed that there was no interaction between experimenters for any of the variables analyzed. The spatial distribution of stimulated loci acquired for each volunteer across the 4 experimenters was analyzed (Fig. 4). It was found that greater spatial area resulted from blinded stimulation trials. A quantitative analysis comparing the improved accuracy of guided versus blind stimulation involved an analysis of 3 dependent variables: (1) the cortical and scalp surface distance of each stimulated loci to the optimal FDI site and (2) the difference in TMS coil twist angle between the original (i.e. the optimal location in the baseline FDI maps at 85%) and subsequent stimulation trials. The calculations were collapsed across the 5 subjects for each of the 4 experimenters. Each of these variables showed the degree to which the experimenters were able to stimulate precise locations a second time, therefore reflecting the spatial accuracy associated with use of the image guided system (Fig. 5).

Comparing cortical distances from each stimulation trial to the optimal location revealed that blindness had a significant effect on spatial accuracy. The guided trials were significantly more accurate spatially than blind trials (main effect of blindness, $F(1, 3) = 170.9$, $Mse = 3.8$, $P < 0.001$) (Fig. 5A). The guided stimulation also conferred a significant improvement in spatial accuracy as judged using distance differences between scalp surface optimal and subsequent stimulation trial locations (main effect of blindness, $F(1, 3) = 199.7$, $Mse = 3.3$, $P < 0.001$) (Fig. 5B). In addition, differences in stimulating coil twist angles between the coil angle used for determining the FDI optimal location and all subsequent stimulation trials were smaller during guided than during blind stimulation (main effect of blindness, $F(1, 3) = 338.3$, $Mse = 1.4$, $P < 0.001$) (Fig. 5C).

The second hypothesis for this study was that improved spatial accuracy would improve response quality by allowing experimenters to stimulate the cortical surface closer to the optimal FDI location. By improved response quality, we refer specifically to: (1) increased probability of eliciting FDI CMAPs from a known optimal location, (2) shorter response latency, (3) larger response amplitude and area, and (4) decreased coefficient of variation for the latter two. The latter two response characteristics were evaluated for all trial response indices where a response was successfully elicited. The response quality was evaluated as a function of blinded condition and TMS stimulation strength.

To evaluate whether the blindness condition affected the probability of eliciting FDI CMAPs, we measured the proportion of trials that produced a response (collapsed across the 5 subjects for each of the 4 experimenters). The overall pattern of results is shown in Fig. 6. The guided trials were significantly more effective at eliciting a response than blind trials (main effect of blindness, $F(1, 3) = 202.1$, $Mse = 12.4$, $P < 0.001$) as were higher power levels (main effect of power, $F(1, 3) = 74.3$, $Mse = 53.0$, $P < 0.01$). In addition to these main effects which reflect the individual contributions of the independent variables, there was a significant interaction between blindness and power ($F(1, 3) = 7.1$, $Mse = 27.5$, $P < 0.05$). To determine the exact source of this interaction, we conducted a set of planned comparisons examining the effect of blindness at each of the 3 power levels. The guided trials were significantly more effective than blind trials at the first and second power levels ($F(1, 3) = 49.2$, $P < 0.001$, and $F(1, 3) = 50.5$, $P < 0.001$, respectively). In contrast, the effect of blindness just missed significance at the third power level ($F(1, 3) = 6.0$, $P = 0.05$).

Comparison of FDI takeoff latencies showed no significant differences across the two blinded conditions. As expected, there was a tendency for latencies to decrease as stimulation strength increased (Fig. 7A).

The CMAPs' amplitude was significantly greater for guided than for blind trials ($F(1, 3) = 22.7$, $P < 0.05$) and was significantly greater as power increased $F(1, 3) = 31.8$, $P < 0.001$). Although blindness and power did not significantly interact with one another, planned comparisons revealed that the effect of blindness was only significant for the second and third power levels ($F(1, 3) = 20.2$, $P < 0.01$, and $F(1, 3) = 16.7$, $P < 0.01$, respectively) (Fig. 7B).

A similar result was obtained for FDI CMAP's area, which was significantly greater for guided than for blind trials (main effect of blindness, $F(1, 3) = 11.2$, $P < 0.05$). Additionally, there was significantly more area under the response curve for trials of increasing power (main effect of power, $F(1, 3) = 31.2$, $P < 0.001$). Although blindness and power did not significantly interact with one another, a series of planned comparisons revealed that the advantage for guided trials over blind trials was significant only for the second and third power levels ($F(1, 3) = 12.2$, $P < 0.05$, and $F(1, 3) = 7.8$, $P < 0.05$, respectively) (Fig. 7C). Therefore, independent of stimulus intensities and particularly at lower stimulation power, the use of the image guided system significantly increased the probability of TMS eliciting a response, which tended to be of larger amplitude and enclosed a larger response area.

Although TMS, using the guided system, was associated with more robust responses, the variability of the response characteristics (i.e. amplitude, and area) was not significantly different from the variability seen during blind stimulation trials. The coefficient of variation obtained for amplitude, and area during blind and guided stimulation is shown in Table 2. Even though logarithmic transformation of these response characteristics reduced the coefficient of variation, the difference between guided and blind stimulation did not achieve statistical significance.

## 4. Discussion

The use of the guided technique in our study was initially developed to aid preoperative planning for patients undergoing neurosurgical procedures. Previous studies using direct electrical stimulation of discrete cortical areas intraoperatively have shown the unreliability of using surface blood vessels and cortical sulci patterns for identifying functional motor cortex. This is a result of the variability in the relationship between cortical surface anatomy and functional cortex (Penfield and Bolder, 1937; Woosley 1947; Penfield and Welch, 1949; Black et al., 1987; Uematsu et al., 1992). Of interest, in the initial mapping phase of our study we observed a similar variability when identifying the optimal FDI cortical representation across

our subjects. Accordingly, an accurate system for guiding TMS stimulation should provide essential information regarding the relationship between functional motor cortex, cortical surface anatomy and pathological lesions as they exist in individual patients. We evaluated the improvements in precision afforded by focal magnetic stimulation when used with a MRI coregistration technique. Taken together, the data for cortical and scalp distance, and twist angle differences provide strong support for the hypothesis that use of the image guided system improves spatial accuracy in re-stimulating specific cortical locations using TMS.

Nielsen (1996a) attempted to improve the precision of coil placement on the scalp by placing volunteers in a chin rest and clamping the stimulating coil so as to stimulate a single scalp location. These authors, however, were not able to quantify any improvement in coil placement precision.

Miranda and coworkers (1997), using a 3-dimensional digitizer for determining the position of the magnetic coil on a volunteer's scalp, showed an improvement in the precision obtained for scalp placement of the coil but were unable to relate stimulated scalp locations to the underlying cortical surface. Wang et al. (1994) reported a head surface digitization technique for coregistering scalp locations onto the MRI cortical surface. The use of a similar technique was developed by our group, which additionally makes use of a laser triangulation system for relating the contours of the scalp and face to the head MRI (Ettinger et al., 1996).

The coregistration system used for our studies not only allows for quantification of coil placement error, but also allows near real time identification of the cortical surface location stimulated by TMS. Additionally, our system affords the volunteer greater comfort during prolonged periods of TMS stimulation because it is an example of a frameless stereotactic system. The benefits accrued from this approach are that volunteers are permitted greater freedom of head movement which affords greater relaxation during stimulation. In addition, visualization of the cortical surface stimulated by TMS resulted in a greater precision of coil placement, which theoretically should decrease the variability of TMS elicited CMAPs.

The second phase of this study, which evaluated this possibility, demonstrated that the probability of eliciting a CMAP at lower stimulation intensity was significantly greater ($P < 0.001$) using visually guided as opposed to blind TMS stimulation of a known optimal cortical location. The significance of this outcome is that low intensity TMS stimulation will excite the lowest threshold motor cortex neuronal clusters during guided stimulation. In order to locate the same cortical locations using blind TMS stimulation would require greater stimulation intensities so as to achieve an equivalent response probability. The greater TMS stimulation strength is coupled with greater spread of induced stimulating currents through the cortex (Pascual-Leone et al., 1994), which might in turn reduce the resolution of the motor cortex functional map. The visually guided TMS induced responses were also significantly more robust with regard to amplitude, and area, at stimulation strengths greater than threshold. The improved CMAP responses using guided stimulation are presumably due to the improved precision with which a coil can be placed for stimulating a motor cortex optimal functional location.

Although these aspects of response quality are improved, the variability of the same response characteristics was not significantly reduced using guided stimulation. It might be argued that audiovisual spontaneous electromyocardiographic (EMG) feedback, not used during data collection, would have reduced the coefficient of variation for CMAP amplitude and area. We do not believe that the use of audiovisual feedback in this study would lead to less variable responses for several reasons. First, spontaneous EMG occurring between the shock artifact and the TMS elicited CMAP was absent. This was true for all stimulation sessions. Secondly, the coefficient of variation found for amplitude and area is in the same range of values noted

in previously published studies where audiovisual feedback was used (Nielsen, 1996a). It would appear that the stimulation protocol used in this study, where volunteers were asked to relax prior to TMS stimulation, achieves the same degree of relaxation observed in previous studies. A third argument involves the fact that the same stimulation protocol was used for both guided and blind stimulation trials. The effect of lack of relaxation of the volunteers would be expected to be the same for both limbs of this study.

Nielsen (1996b) demonstrated that the distribution of TMS induced CMAP amplitude and area are highly skewed. Normalization (using logarithmic transformations) of their data tended to reduce the amplitude and area variability as noted by a reduction of the coefficient of variation for these response parameters. Following their lead, we normalized CMAP parameters acquired during this study. Similar to their results, the coefficient of variation decreased remarkably. Comparing, however, the logarithmically transformed results between visually guided and blind stimulation trials again failed to show a significant reduction in CMAP variability with use of guided stimulation.

It seems likely that large CMAP variability is best explained by physiological changes in both cortical as well as spinal cord neuronal membrane excitability within the cortico-spinal tract motor system. Several studies have demonstrated that pre-movement cognition (Izumi et al., 1995; Ikai et al., 1996), as well as concurrent voluntary changes in muscle tone (Izumi et al., 1996) are among several determinants which affect TMS elicited CMAPs variability. A consensus among previous investigators, concerning the primary focus explaining the observed variability, is still lacking.

It should be emphasized that the accuracy of the coregistration system depends on the accuracy of the hardware, software, and the accuracy of the initial registration procedure, which maps the orientation and position of the subject's head onto a 3-dimensional reconstructed MRI. While both laser scanning and the optical tracking of surface contours can be used for this purpose, the former leads to greater accuracy by virtue of the increased head points available for the registration process. Nevertheless, both techniques can achieve an accuracy of about I mm as reported previously (Ettinger et al., 1996).

The coregistration system in conjunction with focal TMS stimulation techniques was primarily developed for presurgical planning. Its use, however, for studying cortical function is another important application, which should not be overlooked (Pascual-Leone et al., 1999). In this regard, Potts and coworkers have published studies showing the utility of the coregistration system for studying visual function (Potts et al., 1998).

Several other techniques, including positron emission tomography and functional MRI (Wassermann et al., 1996; Krings et al., 1997b), are also available for presurgically locating eloquent cortical areas such as Broca and Wernicke's, which are not directly assessed by TMS at this time. Moreover, the instrumental requirements for the coregistration system used in this study (i.e. MRI and software) are readily available to most clinical or research institutions. This is not always true for the alternate techniques mentioned above. Further, the time resolution for TMS derived functional activity is in the millisecond range and therefore may represent a more accurate preoperative representation of information acquired with direct electrical stimulation of the brain performed during neurosurgical procedures (Penfield and Roberts, 1959). For these reasons, the use of the cortical mapping technique described in this report deserves further exploration.

## Acknowledgments

This research was supported in part by funds from the National Institute of Mental Health Career Investigator Award, including grants K02MH-01110, R01 MH-50747, and by the Scottish Rite Foundation (M.E.S.); by grants PO1

CA67165, R01RR11747 and P41RR13218 (R.K.), and by grant R03 MH60272, and a NARSAD Young Investigator Award (D.T.).

## References

Asanuma, H. The pyramidal tract. In: Brooks, VB., editor. Motor control: handbook of physiology. Vol. 2. Washington, DC: American Physiology Society; 1981. p. 703-733.Sect. 1

Asanuma H, Arnold AP, Zareki P. Further study of the excitation of the pyramidal tract cells by intracortical microstimulation. Exp Brain Res 1976;26:443–461. [PubMed: 1010001]

Barker AT, Jalinous R, Freeston IL. Non invasive magnetic stimulation of the human motor cortex. Lancet 1985;1:1106–1107. [PubMed: 2860322]

Black PM, Ronner SF. Cortical mapping for defining the limits of tumor resection. Neurosurgery 1987;20:914–919. [PubMed: 3614572]

Brasil-Neto JP, McShane LM, Fuhr P, Hallet M, Cohen LG. Topographic mapping of the human motor cortex with magnetic stimulation: factors affecting accuracy and reproducibility. Electroenceph clin Neurophysiol 1992a;85:9–16. [PubMed: 1371748]

Brasil-Neto JP, Cohen L, Panizza M, Nilsson J, Roth BJ, Hallet M. Optimal focal transcranial magnetic activation of the human motor cortex: effects of coil orientation, shape of the induced current pulse, and stimulus intensity. J Clin Neurophysiol 1992b;9:132–136. [PubMed: 1552001]

Brouwer B, Qiao J. Characteristics and variability of lower limb motoneurons responses to transcranial magnetic stimulation. Electroenceph clin Neurophysiol 1995;97:49–54. [PubMed: 7533721]

Cheney PD, Fetz EE. Corticomotoneuronal cells contribute to long latency stretch reflex in the Rhesus monkey. J Physiol 1984;349:249–272. [PubMed: 6737294]

Cohen D, Cuffin N. Developing a more focal magnetic stimulator: part I some basic principles. J Clin Neurophysiol 1991;8:102–111. [PubMed: 2019645]

Cohen LG, Roth BJ, Nilsson J, Dang N, Panizza M, Stefania, Friauf W, Hallet M. Effects of coil design on delivery of focal magnetic stimulation: technical considerations. Electroenceph clin Neurophysiol 1990;75:350–357. [PubMed: 1691084]

Cohen LG, Bandinelli S, Findley TW, Hallet M. Motor reorganization after upper limb amputation in man. Brain 1991a;114:615–627. [PubMed: 2004259]

Cohen LG, Roth BJ, Wassermann EM, Topka H, Fuhr P, Schultz J, Hallet M. Magnetic stimulation of the human cerebral cortex an indicator of reorganization in motor pathways in certain pathological conditions. J Clin Neurophysiol 1991b;8:56–65. [PubMed: 2019651]

Cohen L, Brasil-Neto J, Pascual-Leone A, Hallet M. Plasticity of cortical motor output organization following deafferentation cerebral lesions and skill acquisition. Adv Neurol 1993;63:187–200. [PubMed: 8279304]

Ellaway PH, Davey NJ, Maskill DW, Rawlinson SR, Lewis HS, Anissimova NP. Variability in the amplitude of skeletal muscle responses to magnetic stimulation of the motor cortex in man. Electroenceph clin Neurophysiol 1998;109:104–113. [PubMed: 9741800]

Ettinger, GJ.; Grimson, WEL.; Leventon, ME.; Kikinis, R.; Gugino, V.; Cote, W.; Karapelou, M.; Aglio, L.; Shenton, M.; Potts, G.; Alexander, E. Non invasive functional brain mapping using registered transcranial magnetic stimulation. IEEE Workshop on mathematical methods in biomedical image analysis; San Francisco, CA. June 21–22; 1996.

Fadiga L, Fogassi L, Pavesi G, Rizzolatti G. Motor facilitation during action observation: a magnetic stimulation study. J Neurophysiol 1995;73:2608–2611. [PubMed: 7666169]

Grimson WEL, Kikinis R, Jolesz FA, Black PMcL. Image-guided surgery. Sci Am 1999;2:2–9.

Gugino, LD.; Potts, G.; Aglio, LS.; Alexander, E., III; Grimson, WEL.; Kikinis, R.; Shenton, M.; Black, PMcL; Ettinger, GJ.; Cote, WA.; Leventon, M.; Gonzalez, AA. Localization of eloquent cortex using transcranial magnetic stimulation. In: Alexander, E., III; Levy Maciunas, J., editors. Advanced neurosurgical navigation. New York, NY: Thieme Medical Publishers; 1999. p. 163-199.

Horn BKP. Closed-form solution of absolute orientation using unit quaternions. J Opt Soc Am A 1987;4:629–642.

Izumi, Shin-Ichi; Findley, TW.; Ikai, T.; Andrews, J.; Daum, M.; Chino, N. Facilitatory effect of thinking about movement on motor evoked potentials to transcranial magnetic stimulation of the brain. Am J Phys Med Rehab 1995;74:207–213.

Izumi, Shin-Ichi; Findley, TW.; Andrews, JF.; Daum, MC.; Chino, N. Voluntary contraction shortens peripheral conduction time in response to transcranial magnetic stimulation of the brain. Electroenceph clin Neurophysiol 1996;101:329–333. [PubMed: 8761042]

Kapur, T.; Grimson, WEL.; Kikinis, R. Segmentation of brain tissue from MR images. Proceedings of the First International Conference on computer vision, Virtual Reality and Robotics in Medicine; Nice, France. Apr. 1995 p. 429-433.

Kiers L, Cros D, Chiapa KH, Fang J. Variability of motor potentials evoked by transcranial magnetic stimulation. Electroenceph clin Neurophysiol 1993;89:415–423. [PubMed: 7507428]

Krings T, Buchbinder BR, Butler WE, Chiapa KH, Jiang HJ, Rosen BR, Cosgrove GR. Stereotactic transcranial magnetic stimulation: correlation with direct electrical cortical stimulation. Neurosurgery 1997a;41:1319–1326. [PubMed: 9402583]

Krings T, Buchbinder BR, Butler WE, Chiapa KH, Jiang HJ, Cosgrove GR, Rosen BR. Functional magnetic resonance imaging and transcranial magnetic stimulation: complementary approaches in the evaluation of cortical motor function. Neurology 1997b;48:1406–1416. [PubMed: 9153482]

Levy WJ, Amassian VF, Traad M, Cadwell J. Focal magnetic coil stimulation reveals motor cortical system reorganized in humans after traumatic quadriplegia. Brain Res 1990;510:130–134. [PubMed: 2322837]

Levy WJ, Amassian VE, Schmid UD, Junrgeis C. Mapping of motor cortex gyral sites non invasively by transcranial magnetic stimulation in normal subjects and patients. Magnetic motor stimulation: basic principles and clinical experience. Electroenceph clin Neurophysiol 1991;43(Suppl):51–75.

Miranda Cavaleiro P, Mamede de Carvaho, Conceiçao I, Sales Luis ML, Ducla-Soares E. A new method for reproducible coil positioning in transcranial magnetic stimulation mapping. Electroenceph clin Neurophysiol 1997;105:116–123. [PubMed: 9152204]

Mortifee P, Stewart H, Schultzer M, Eisen A. Reliability of transcranial magnetic stimulation for mapping the human motor cortex. Electroenceph clin Neurophysiol 1994;93:131–137. [PubMed: 7512919]

Nielsen JF. Improvement of amplitude variability of motorevoked potentials in multiple sclerosis patients and in healthy subjects. Electroenceph clin Neurophysiol 1996a;101:404–411. [PubMed: 8913193]

Nielsen JF. Logarithmic distribution of amplitudes of compound muscle action potentials evoked by transcranial magnetic stimulation. J Clin Neurophysiol 1996b;13:423–434. [PubMed: 8897207]

Nielsen J, Petersen N. Changes in the effect of magnetic brain stimulation accompanying voluntary dynamic contraction in man. J Physiol 1995;484:777–789. [PubMed: 7623292]

Oldfield RC. The assessment and analysis of handedness. J Clin Psychol 1974;30:545–552. [PubMed: 4422570]

Pascual-Leone A, Valls-Solé J, Wassermann EM, Hallet M. Responses to rapid-rate transcranial magnetic stimulation of the human motor cortex. Brain 1994;117:847–858. [PubMed: 7922470]

Pascual-Leone A, Bartres-Faz D, Keenan JP. Transcranial magnetic stimulation: studying the brain–behaviour relationship by induction of ‘virtual lesions’. Philos Trans R Soc Lond Biol Sci 1999;354:1229–1238. [PubMed: 10466148]

Penfield W, Bolder P. Somatic motor and sensory representation in the cerebral cortex of man as studied by electrical stimulation. Brain 1937;60:389–443.

Penfield, W.; Roberts, R. Speech and brain mechanisms. Princeton, NJ: Princeton University Press; 1959.

Penfield W, Welch K. Instability of response to stimulation of the sensorimotor cortex of man. J Physiol 1949;109:358–365. [PubMed: 15395018]

Potts GF, Gugino LD, Leventon ME, Grimson WE, Kikinis R, Cote W, Alexander E, Anderson JE, Ettinger GJ, Aglio LS, Shenton ME. Visual hemifield mapping using transcranial magnetic stimulation coregistered with cortical surfaces derived from magnetic resonance images. J Clin Neurophysiol 1998;15:344–350. [PubMed: 9736468]

Shenton, ME.; Kikinis, R.; McCarley, RW.; Saiviroonporn, P.; Hokama, HH.; Robatino, A.; Metcalf, D.; Wible, CG.; Portas, CM.; Losifescu, DV.; Donnino, R.; Goldstein, JM.; Jolesz, FA. Harvard brain atlas: a teaching and visualization tool. Proceedings of the 1995 biomedical visualization; Atlanta, GA. Oct 30. 1995 p. 10-17.

Thickbroom GW, Byrnes ML, Mastaglia FL. A model of the effect of MEP amplitude variation on the accuracy of TMS mapping. Clin Neurophysiol 1999;110:941–943. [PubMed: 10400209]

Traversa R, Cicinelli P, Bassi A, Rossini PM, Bernardi G. Mapping of motor cortical reorganization after stroke. Stroke 1997;28:110–117. [PubMed: 8996498]

Triggs WJ, Subramanium B, Rossi F. Hand preference and transcranial magnetic stimulation asymmetry of cortical motor representation. Brain Res 1999;835:324–329. [PubMed: 10415389]

Uematsu S, Lesser R, Fisher RS, Gordon B, Hara K, Krauss GL, Vining EP, Webber RW. Motor and sensory cortex in humans: topography studied with chronic subdural stimulation. Neurosurgery 1992;31:59–72. [PubMed: 1641111]

Wang C, Pahl JJ, Hogue RE. A method for co-registering three-dimensional multi-modality brain images. Comput Methods Programs Biomed 1994;44:131–140. [PubMed: 7988116]

Wassermann EM, McShane LM, Hallet M, Cohen L. Non invasive mapping of muscle representations in human motor cortex. Electroenceph clin Neurophysiol 1992;85:1–8. [PubMed: 1371738]

Wassermann EM, Wang B, Zeffiro TA, Sadato N, Pascual-Leone A, Toro C, Hallet M. Locating the motor cortex on the MRI with transcranial magnetic stimulation and PET. NeuroImage 1996;3:1–9. [PubMed: 9345470]

Woosley CN. Patterns of sensory representation in the cerebral cortex. Fed Proc 1947;6:437–441. [PubMed: 20262562]

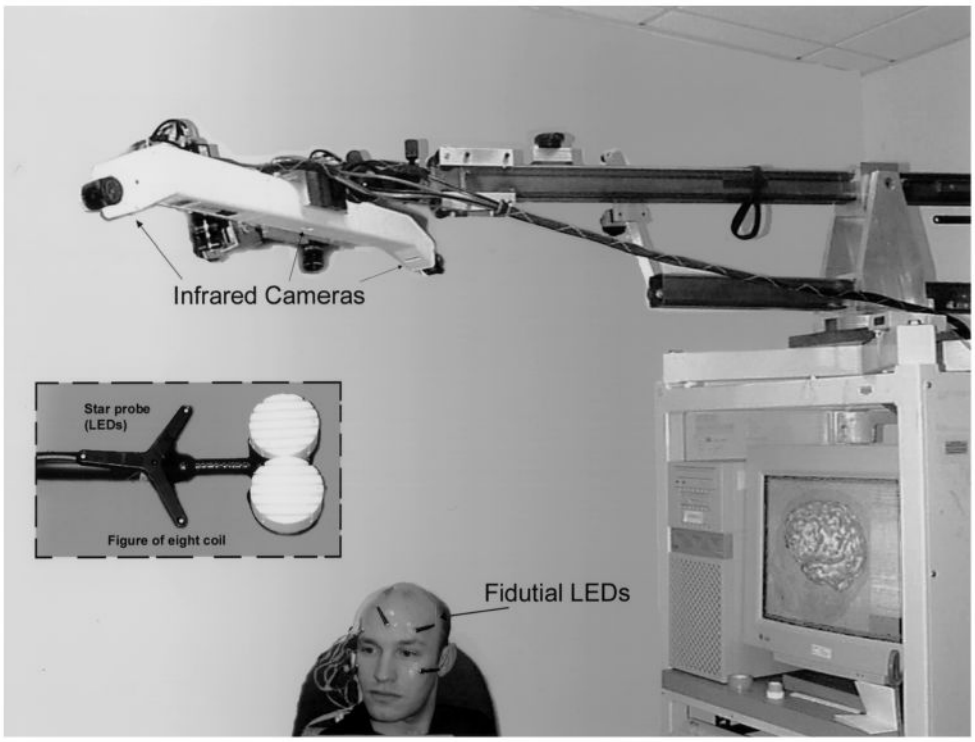


**Fig. 1.**

Diagram of experimental setup used for guided focal TMS. The volunteer is shown with LEDs fixed to the maxillary and forehead regions. Light flashes emitted by the LEDs, which serve as fiducials, are registered by the infrared cameras above. The star probe attached to the figure of 8 coil also has LEDs for determining the relative position of the stimulating coil to the scalp. Both the pixsys system (i.e. optical tracking system) and laser scanner used for the initial coregistration are attached to the boom overlying the volunteer's head.

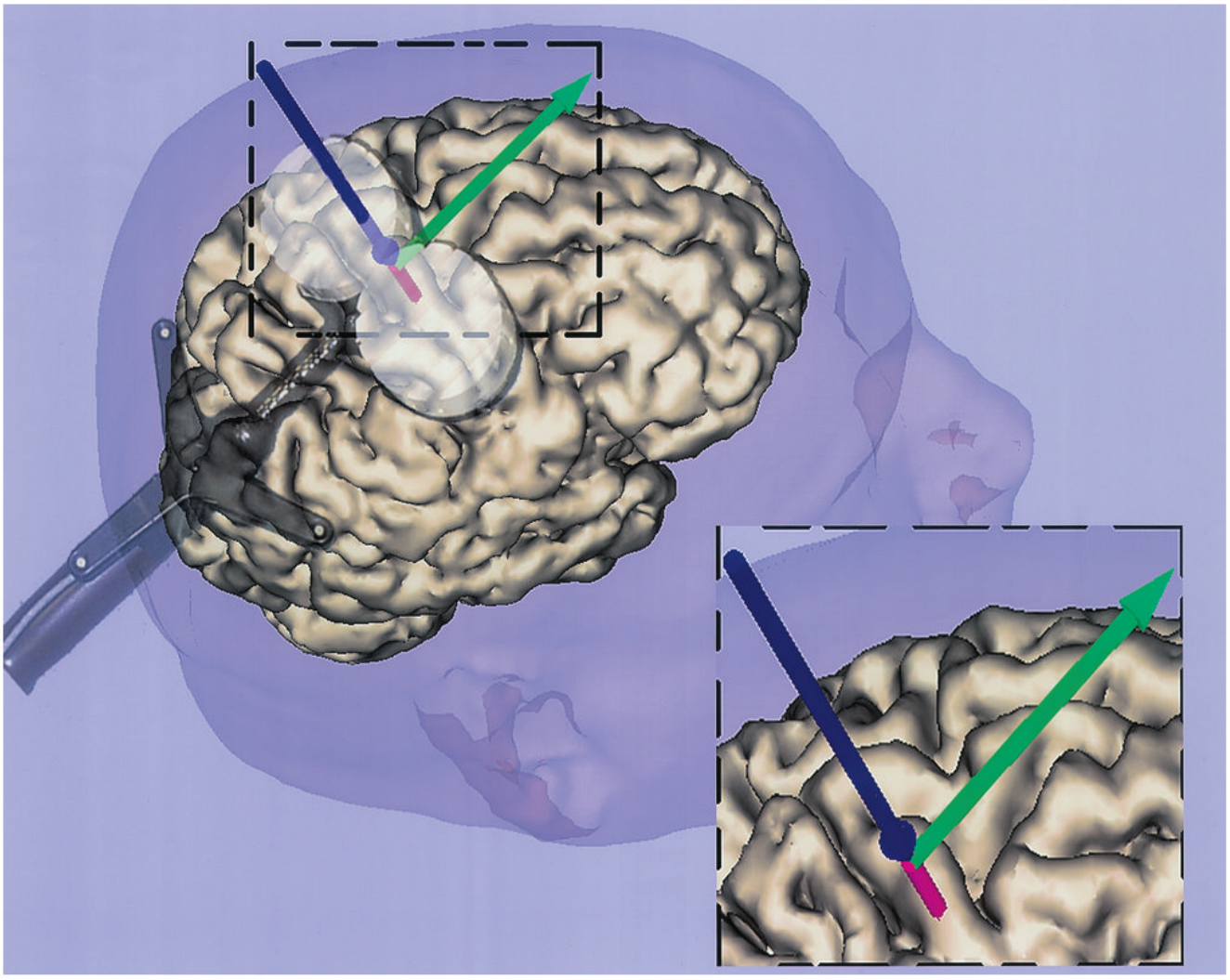

**Fig. 2.**

An example of the live display (insert at lower right corner of figure) showing the location of the cortical surface intersected by the peak TMS induced electric field (shown as the red extension beyond the vertical blue line). The spherical expansion at the bottom of the blue line represents the scalp intersection. The green arrow shows the degree of twist angle for each scalp placement of the TMS coil. The double circular coil is placed on the scalp.

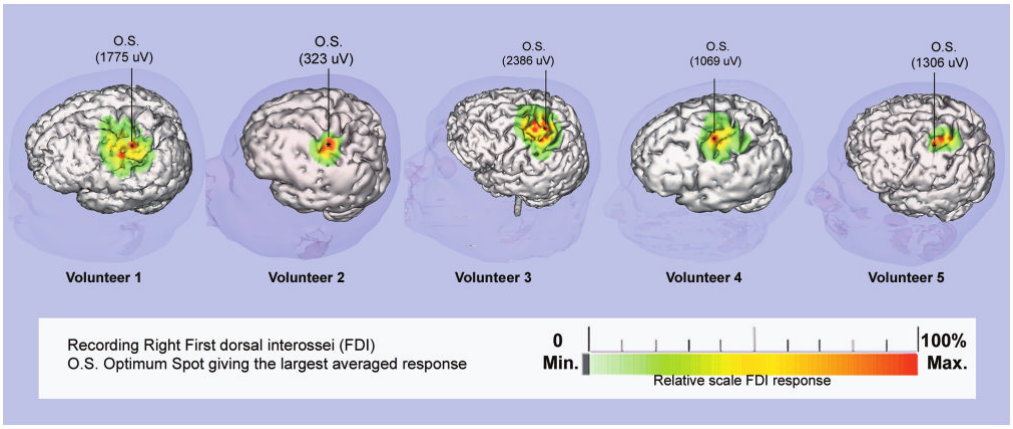


**Fig. 3.**

Motor area topographical maps for the right FDI muscle obtained from data using focal TMS with the coregistration system. The cortical surface area which when stimulated produced FDI CMAPs is color-coded as a function of CMAP amplitude. A single 4-point linear interpolation is used for assigning amplitude values between stimulated locations. The relative color scale below is normalized to the maximum CMAP amplitude acquired during the mapping session. The optimal FDI location was defined as the stimulated site leading to the maximum averaged CMAP amplitude.

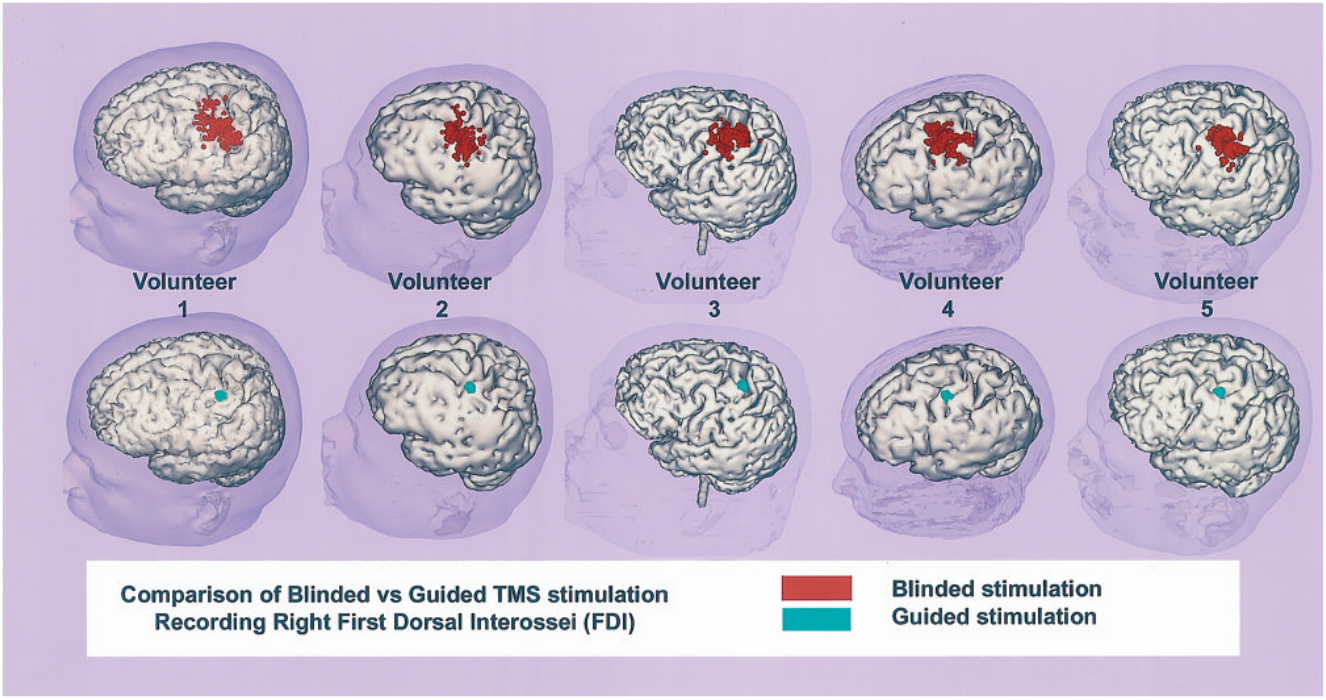


**Fig. 4.**
Comparison of stimulated cortical surface areas using blind (red spots upper row) versus guided stimulation (green spots lower row of virtual brains). The results shown for each volunteer are arranged as columns of virtual brains.

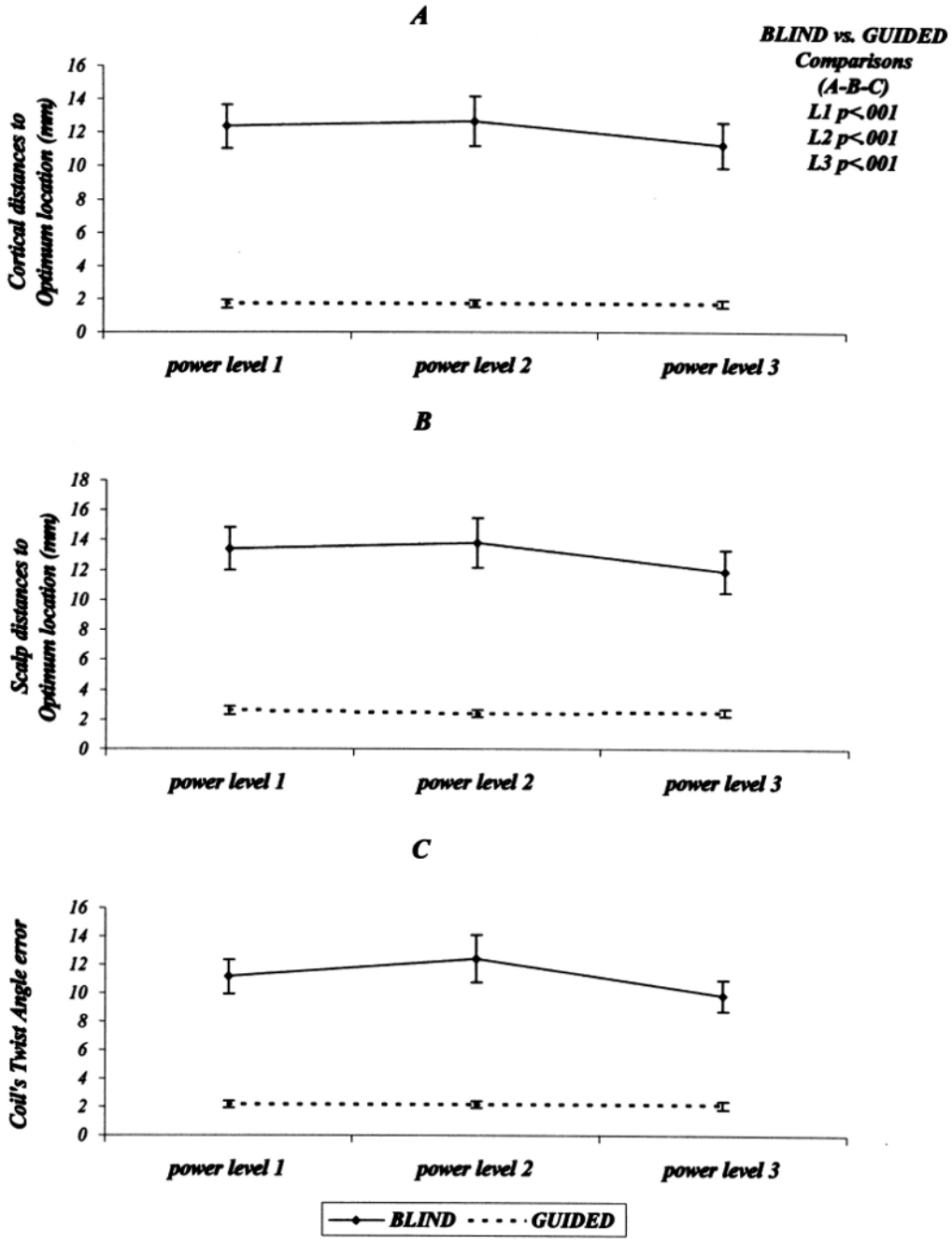


**Fig. 5.**

(A) Plots of the averaged stimulated cortical surface location distances to the optimal FDI location as a function of stimulus intensity. The upper plot (continuous line) represents this relationship for blind stimulation. The lower plot (interrupted line) represents the same descriptors acquired during guided stimulation. (B) Plots for spatial distance to the FDI optimal location on the scalp. (C) Plots for the twist angle difference (error) between blind and guided stimulation. Error bars represent the 95% confidence limits.

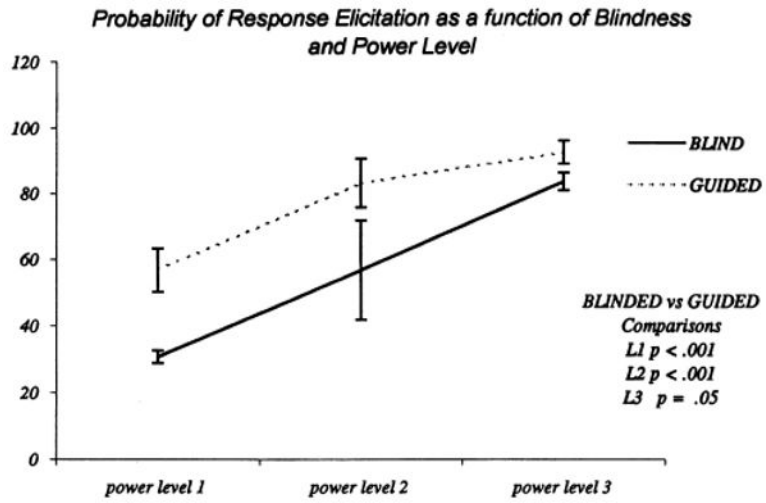


**Fig. 6.**

Plots of response probability at the 3 TMS stimulation intensities. The continuous line shows the results acquired during blind stimulation while the interrupted line shows guided stimulation results. Error bars represent the 95% confidence limits.

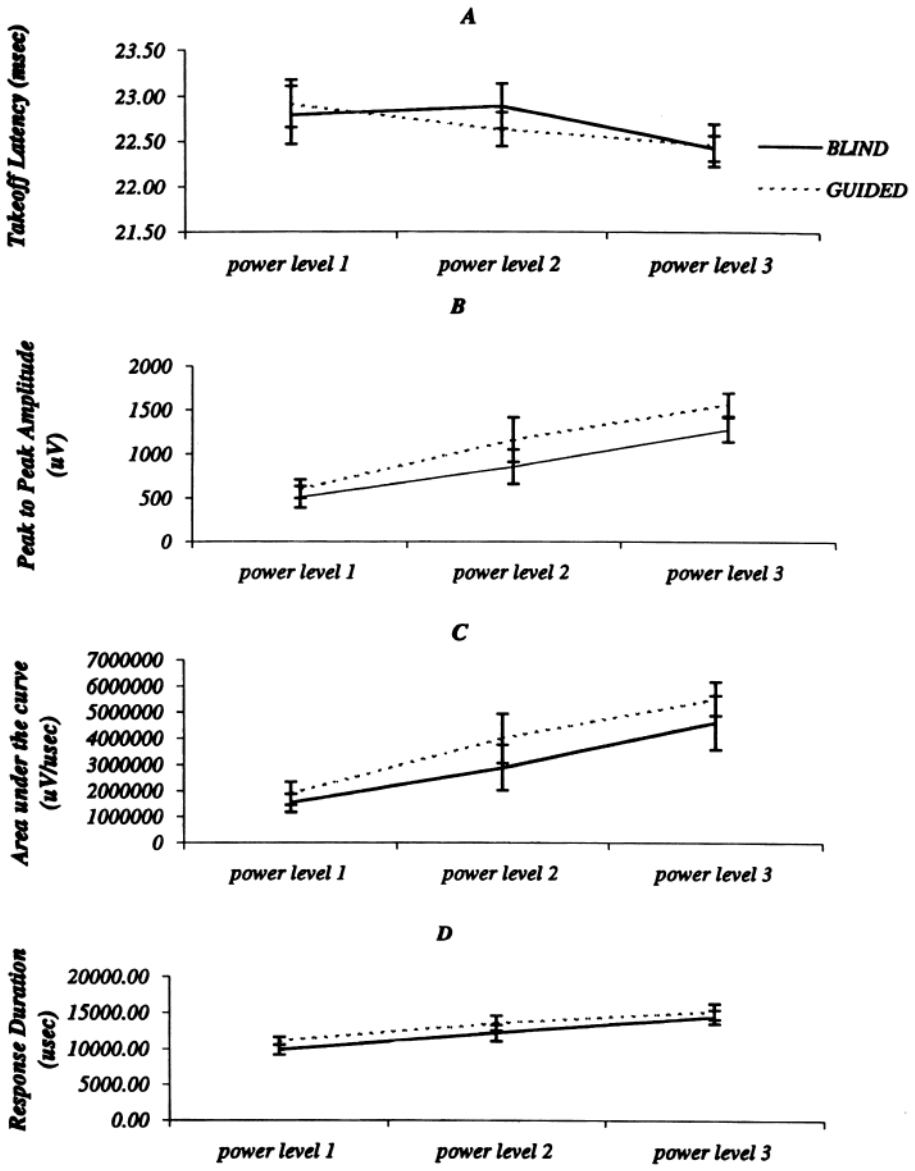


**Fig. 7.**

Comparison of response descriptors across blinded condition and TMS stimulation intensities: (A) takeoff latency, (B) peak-to-peak amplitude, and (C) area. Results acquired for the blind condition are shown using continuous lines whereas guided stimulation results are depicted using interrupted lines. Error bars represent the 95% confidence limits.

## Table 1

Comparison of the resting motor threshold (rMT) of each subject to absolute intensity (power levels 1, 2, and 3) of the stimulator output used

| | Power level 1[a] | Power level 2[b] | Power level 3[c] | Mapping phase intensity (85%)[d] |
|---|---|---|---|---|
| Subject 1 | 70 | 1.2 | 1.4 | 1.2 |
| Subject 2 | 78 | 1.1 | 1.3 | 1.1 |
| Subject 3 | 66 | 1.3 | 1.5 | 1.3 |
| Subject 4 | 68 | 1.2 | 1.5 | 1.2 |
| Subject 5 | 72 | 1.2 | 1.4 | 1.2 |

[a] Power level 1 equals rMT, and is expressed as % of magnetic stimulator output.

[b] Power level 2 represents an intermediate intensity between rMT and 100% of the stimulator output, and is expressed relative to rMT (i.e. rMT times).

[c] Power level 3 represents 100% of the stimulator output, and is expressed relative to rMT (i.e. rMT times).

[d] Mapping phase intensity is expressed relative to rMT (i.e. rMT times).

**Table 2**

Comparison of the averages of coefficients of variation of response descriptors between blindness condition and TMS stimulation intensity level

| | Not log transformed | | | Log transformed | | |
|---|---|---|---|---|---|---|
| | **Area** | **Amplitude** | **Response duration** | **Area** | **Amplitude** | **Response duration** |
| Blind-level 1 | 1.02 | 0.89 | 0.30 | 0.06 | 0.13 | 0.27 |
| Blind-level 2 | 0.67 | 0.58 | 0.25 | 0.05 | 0.10 | 0.22 |
| Blind-level 3 | 0.63 | 0.55 | 0.25 | 0.05 | 0.10 | 0.22 |
| Guided-level 1 | 0.81 | 0.72 | 0.26 | 0.05 | 0.10 | 0.22 |
| Guided-level 2 | 0.64 | 0.51 | 0.30 | 0.05 | 0.10 | 0.25 |
| Guided-level 3 | 0.49 | 0.40 | 0.24 | 0.04 | 0.07 | 0.20 |